

See discussions, stats, and author profiles for this publication at: <https://www.researchgate.net/publication/260108239>

1 α ,25-Dihydroxyvitamin D₃ Modulates CYP2R1 Gene Expression in Human Oral Squamous Cell Carcinoma Tumor Cells

ARTICLE *in* HORMONES AND CANCER · FEBRUARY 2014

Impact Factor: 0.02 · DOI: 10.1007/s12672-014-0170-5 · Source: PubMed

CITATIONS

5

READS

46

5 AUTHORS, INCLUDING:



Yuvaraj Sambandam

Medical University of South Carolina

15 PUBLICATIONS 220 CITATIONS

SEE PROFILE



Carol L Wagner

Medical University of South Carolina

147 PUBLICATIONS 4,274 CITATIONS

SEE PROFILE



Sakamuri V Reddy

Medical University of South Carolina

100 PUBLICATIONS 2,957 CITATIONS

SEE PROFILE

1 α ,25-Dihydroxyvitamin D3 Modulates CYP2R1 Gene Expression in Human Oral Squamous Cell Carcinoma Tumor Cells

Kumaran Sundaram · Yuvaraj Sambandam ·
Eichi Tsuruga · Carol L. Wagner · Sakamuri V. Reddy

Received: 25 November 2013 / Accepted: 22 January 2014
© Springer Science+Business Media New York 2014

Abstract Oral squamous cell carcinomas (OSCC) are the most common malignant neoplasms associated with mucosal surfaces of the oral cavity and oropharynx. 1 α ,25-Dihydroxyvitamin D3 (1,25(OH)₂D3) is implicated as an anticancer agent. Cytochrome P450 2R1 (CYP2R1) is a microsomal vitamin D 25-hydroxylase which plays an important role in converting dietary vitamin D to active metabolite, 25-(OH)D3. We identified high levels of CYP2R1 expression using tissue microarray of human OSCC tumor specimens compared to normal adjacent tissue. Therefore, we hypothesize that 1,25(OH)₂D3 regulates CYP2R1 gene expression in OSCC tumor cells. Interestingly, real-time RT-PCR analysis of total RNA isolated from OSCC cells (SCC1, SCC11B, and SCC14a) treated with 1,25(OH)₂D3 showed a significant increase in CYP2R1 and vitamin D receptor (VDR) mRNA expression. Also, Western blot analysis demonstrated that 1,25(OH)₂D3 treatment time-dependently increased CYP2R1 expression in these cells. 1,25(OH)₂D3 stimulation of OSCC cells transiently transfected with the hCYP2R1 promoter (−2 kb)-luciferase reporter plasmid demonstrated a 4.3-fold increase in promoter activity. In addition, 1,25(OH)₂D3 significantly increased c-Fos, p-c-Jun expression, and c-Jun N-terminal kinase (JNK) activity in these cells. The JNK inhibitor suppresses 1,25(OH)₂D3, inducing CYP2R1 mRNA expression and gene promoter activity in OSCC cells. Furthermore, JNK inhibitor significantly decreased 1,25(OH)₂D3 inhibition of OSCC tumor cell proliferation. Taken together, our results suggest that AP-1 is a downstream effector of 1,25(OH)₂D3 signaling to modulate CYP2R1 gene expression in OSCC tumor cells, and vitamin

D analogs could be potential therapeutic agents to control OSCC tumor progression.

Introduction

Head and neck squamous cell carcinoma (HNSCC) contributes to approximately 3 % of all malignancies in the USA [25]. More than 90 % of oral cancers are squamous cell carcinomas (OSCC) which contributes >40 % of HNSCC and are associated with mucosal surfaces of the oral cavity and oropharynx [18]. The etiology of OSCC is strongly associated with certain environmental, lifestyle risk factors including tobacco, alcohol consumption, chronic inflammation, and viral infections. Genetic alteration and molecular events such as cytogenic abnormalities, inactivation of tumor suppressor genes, and changes in intracellular signaling pathways are involved in OSCC tumor progression [39]. OSCC show a potent activity of local bone invasion, which dramatically impacts the patients' recovery and quality of life [32]. OSCC tumor cells have been shown to invade maxillary and mandibular bone in a murine model [28]. It has been reported that TGF- β signaling in the tumor–bone microenvironment facilitates cancer cell invasion of bone [15]. Nuclear factor kappaB (NF- κ B) expression is upregulated in OSCC gradually from premalignant lesions to invasive cancer [26]. It has been shown that MMP-1 and MMP-9 are highly expressed in BHY cells, derived from an SCC which had deeply invaded into the mandible [10]. Some of the chemoattractants present in the bone matrix play a pivotal role in bone invasion. Recently, we demonstrated that CXCL13 plays an important role in OSCC invasion of bone/osteolysis in athymic mice [29].

1 α ,25-Dihydroxyvitamin D3 (1,25(OH)₂D3; calcitriol) is the most biologically active form of vitamin D metabolite with

K. Sundaram · Y. Sambandam · E. Tsuruga · C. L. Wagner ·
S. V. Reddy (✉)
Charles P. Darby Children's Research Institute, Medical University
of South Carolina, 173 Ashley Avenue, Charleston, SC 29425, USA
e-mail: reddysv@musc.edu

high affinity to the vitamin D receptor (VDR) and has been implicated as an anticancer agent [23]. Previously, it has been reported that vitamin D3 and 13-*cis* retinoic acid have equipotent antiproliferative effects on tongue squamous cell carcinoma (SCC-25) cells [9]. Also, 1,25(OH)₂D3 has been shown to inhibit the growth of HNSCC cells through upregulation of cell cycle inhibitor p18 expression [14]. Single nucleotide polymorphisms associated with VDR have been shown to increase the risk of OSCC [24]. Vitamin D 25-hydroxylase (CYP2R1) is a member of the cytochrome P450 superfamily of monooxygenases, which are involved in drug metabolism and synthesis of cholesterol, steroids, and lipids. CYP2R1 is a microsomal enzyme that converts vitamin D into 25-(OH)D3 [4]. The physiologic significance of CYP2R1 was established by the finding in two Nigerian brothers that a homologous inactivating L99P mutation of the *CYP2R1* gene was associated with rickets caused by isolated 25(OH)D deficiency [4]. In this study, we demonstrated CYP2R1 expression and 1,25(OH)₂D3 transcriptional regulatory mechanism in oral squamous cell carcinoma tumor cells.

Materials and Methods

Reagents and Antibodies Cell culture and DNA transfection reagents were purchased from Invitrogen (Carlsbad, CA). 1,25(OH)₂D3 was purchased from Enzo Life Sciences (Farmingdale, NY). Anti-CYP2R1, anti-c-Fos, anti-p-c-Jun, and peroxidase-conjugated secondary antibodies were purchased from Santa Cruz Biotechnology (Santa Cruz, CA). Supersignal enhanced chemiluminescence (ECL) reagent was obtained from Amersham Bioscience (Piscataway, NJ), and nitrocellulose membranes were purchased from Millipore (Bedford, MA). A luciferase reporter assay system was obtained from Promega (Madison, WI). Protease inhibitor cocktail was purchased from Sigma Chemical Co. (St. Louis, MO), and c-Jun N-Terminal Kinase (JNK) inhibitor (SP600125) was purchased from Calbiochem (San Diego, CA).

Cell Lines and Cell Cultures Human OSCC-derived cell lines SCC1, SCC11B, and SCC14a were generously provided by Dr. Thomas E. Carey (University of Michigan, Ann Arbor, MI) and were maintained in Dulbecco's Modified Eagle's Medium (DMEM) containing 10 % fetal bovine serum (FBS) and supplemented with L-glutamine, penicillin, and streptomycin. All cells were incubated at 37 °C in 5 % CO₂.

Quantitative Real-Time Reverse Transcription PCR CYP2R1 mRNA expressions in OSCC cells were measured by real-time reverse transcription (RT)-PCR as described previously [34]. Briefly, total RNA was isolated from human OSCC cells stimulated with and without 1,25(OH)₂D3 (10⁻⁸ M) for 0–48 h, using

RNAzol reagent (Biotech Labs, Houston, TX). A reverse transcription reaction was performed using poly-dT primer and reverse transcriptase in a 25-μl reaction volume containing total RNA (2 μg), 1× PCR buffer and 2 mM MgCl₂, at 42 °C for 15 min and followed by 95 °C for 5 min. The quantitative real-time PCR was performed using IQTM SYBR Green Supermix in an iCycler (iCycler iQ Single-Color Real-Time PCR Detection System; Bio-Rad, Hercules, CA). The primer sequences used to amplify the human glyceraldehyde-3-phosphate dehydrogenase (GAPDH) mRNA were 5' CCTACCCCAATGTATCCGTTG TG-3' (sense) and 5'-GGAGGAATGGGAGTTGCTGTTGAA-3' (antisense); human CYP2R1 mRNA were 5' GAAAGCAG AGCCAGGTGTACG 3' (sense) and 5' TCATGAATAAAGGA AGGCATGG 3' (antisense); and human VDR mRNA were 5' CCAACTCCAGACACACTCC 3' (sense) and 5' AGATTG GAGAAGCTGGACGA 3' (antisense). Thermal cycling parameters were 94 °C for 3 min, followed by 40 cycles of amplifications at 94 °C for 30 s, 60 °C for 1 min, 72 °C for 1 min, and 72 °C for 5 min as the final elongation step. Relative levels of CYP2R1 mRNA expression were normalized in all the samples analyzed with respect to GAPDH amplification.

Cloning and Characterization of hCYP2R1 Gene Promoter The CYP2R1 gene promoter region (−1 to −2 kb relative to the transcription start site) was PCR-amplified using the template human genomic DNA and CYP2R1 gene-specific primers, 5'-GAGCTCGAGTTATTGATTAA TAAGAATTTT-3' (sense) and 5'-GAGCTCGAGCGGCC CGAGCTGGAGCTGGAGGTGCGAAC-3' (antisense) (GenBankTM accession no. AY800276.1). Sequences underlined are the XhoI restriction enzyme site added for subcloning purposes. The PCR-amplified CYP2R1 promoter fragment was subcloned into the pGL2 Basic vector, and the resulting plasmid termed pGL2 Basic-hCYP2R1-luciferase and the promoter sequence were analyzed using the web-based TF database search.

SCC14a cells were cultured in DMEM supplemented with 10 % FBS and 100 units/ml of penicillin/streptomycin. DNA transfections were performed using Lipofectamine-Plus transfection reagent (Invitrogen, Inc., San Diego, CA). Cells were transiently transfected with pGL2 Basic-hCYP2R1-luciferase plasmid and cultured in the presence or absence of 1,25 (OH)₂D3 (10⁻⁸ M) for 48 h. A 20-μl aliquot of total cell lysates was mixed with 100 μl of the luciferase assay reagent. The light emission was measured for 10 s of integrated time using Sirius Luminometer following the manufacturer's instructions (Promega, Madison, WI). The transfection efficiency was normalized by co-transfection with pRSV β-gal plasmid and measuring the β-galactosidase activity in these cells.

Tissue Microarray Tissue microarray (TMA) of 60 primary human OSCC tumor specimens were obtained from the Head and Neck Cancer Tissue Array Initiative at the NIDCR, NIH

[27], and 14 control adjacent normal tissues were obtained from the Hollings Cancer Center Tissue Biorepository, Medical University of South Carolina, in accordance with an Institutional Review Board (IRB)-approved protocol. Serial 5- μ m sections were cut on a modified Leica RM 2155 rotary microtome (Leica Microsystems, Richmond Hill, ON, Canada). TMA blocks were deparaffinated in xylene for 10 min and rehydrated by successive transfers in alcohol with decreasing concentration and finally in H₂O. Then, sections were washed for 5 min in 3 % H₂O₂ to inhibit endogenous peroxidase. The slides were incubated with goat polyclonal antibody against CYP2R1 for 3 h at room temperature. Immunohistochemical (IHC) staining was performed with HRP-labeled secondary antibody and diaminobenzidine (Vector Laboratories, Burlingame, CA, USA). The slides were briefly counterstained with hematoxylin and dehydrated through graded alcohols to xylene and were cover slipped with a permanent mounting media. CYP2R1 IHC semiquantification was determined using the modified *H* score which consists of the sum of percent of tumor cells staining multiplied by an ordinal value corresponding to the staining intensity level (0=none, 1=weak, 2=moderate, and 3=strong). IHC scores were determined by taking the product of the estimated staining intensity and area of tissue (tumor or normal) stained ($<1/3=1$; $1/3-2/3=2$; $>2/3=3$), giving a range of possible scores between 0 and 9. IHC scores were averaged to determine a composite score for each group as described [19].

Cell Proliferation Assay OSCC tumor cells were stimulated with 1,25(OH)₂D3 (10^{-8} M) alone and in the presence of a 2- μ M concentration of JNK inhibitor (SP600125) for 24 h, then incubated with alamarBlue reagent (Life technologies, Grand Island, NY) for 4 h at 37 °C. The fluorescence intensity was read at 560 nm of excitation and at 590 nm of emission, and alamarBlue reduction was calculated as per the manufacturer's protocol. Background absorbance was subtracted using a control media.

Western Blot Analysis OSCC cells were stimulated with 1,25(OH)₂D3 (10^{-8} M) for an indicated time point (0–72 h) and lysed in a buffer containing 20 mM Tris-HCl at pH 7.4, 1 % Triton X-100, 1 mM EDTA, 1.5 mM MgCl₂, 10 % glycerol, 150 mM NaCl, and 0.1 mM Na₃VO₄. The protein content of the samples was measured using the BCA protein assay reagent (Thermo Fisher Scientific Inc., Rockford, IL). Protein (20 μ g) samples were then subjected to SDS-PAGE using 12 % Tris-HCl gels and blot transferred onto a nitrocellulose membrane and immunoblotted with anti-CYP2R1, anti-c-Fos, and anti-p-c-Jun antibodies. The bands were detected using the enhanced chemiluminescence detection system. The band intensity was quantified by densitometric analysis using the NIH ImageJ Program.

JNK Activity Assay SCC14a cells were stimulated with 1,25(OH)₂D3 (10^{-8} M) for 0–6 h. Cells were resuspended in cell lysis buffer (20 mM Tris (pH 7.4), 150 mM NaCl, 1 mM EDTA, 1 mM EGTA, 2.5 mM sodium pyrophosphate, 1 mM β -glycerol phosphate, 1 mM sodium vanadate, 1 μ g/ml leupeptin, 1 mM phenylmethyl sulfonyl fluoride (PMSF), and 1 % Triton X-100), followed by a brief sonication. Cell lysates were cleared by centrifugation for 3 min at 1,200g, and the supernatants were assayed for N-terminal JNK activity using a solid-phase GST-c-Jun (1–89 amino acids) fusion protein. Briefly, JNK was co-precipitated with its substrate conjugated to glutathione-S-sepharose beads at 4 °C. After overnight incubation, the precipitates were washed twice with cell lysis buffer followed by a kinase buffer (25 mM Tris (pH 7.5), 5 mM β -glycerol phosphate, 1 mM sodium vanadate, 2 mM dithiothreitol (DTT), and 10 mM MgCl₂). After the last wash, pellets were resuspended in 50 μ l of kinase buffer. The reaction was carried out at 30 °C for 30 min in the presence of 100 μ M of ATP and stopped by adding sample buffer. Proteins were separated by SDS-PAGE (15 %) and blot transferred onto a nitrocellulose membrane. p-c-Jun expression was detected with a specific anti-phospho-c-Jun antibody following the manufacturer's instructions (New England Biolabs, Beverly, MA, USA).

Statistical Analysis Results are presented as mean \pm SD for three independent experiments and were compared by Student's *t* test. Paired *t* test was used to compare the mean *H* score of CYP2R1 levels in OSCC and normal adjacent tissues. Values were considered significantly different for $p<0.05$.

Results

CYP2R1 Expression in Oral Squamous Cell Carcinoma

Cytochrome P450 (CYP) enzymes play an important role in the conversion of inactive vitamin D into active 1,25(OH)₂D3. CYP2R1 catalyzes the initial step converting vitamin D into 25-hydroxyvitamin D3 (25-(OH)D3) in the liver. It has been shown that several cancer cell types are capable of producing 1,25(OH)₂D3 to regulate their growth [33]. Therefore, we examined the CYP2R1 abundance in OSCC tumor specimens. Interestingly, immunohistochemical staining using a TMA of 60 human OSCC tumor specimens identified that 56 of 60 (>90 %) stained strongly positive for CYP2R1 abundance with an average *H* score >7 as described in “Materials and Methods.” In contrast, 14 normal adjacent tissues demonstrated very low levels of CYP2R1 expression with an average *H* score <2. A representative OSCC tumor specimen demonstrated an abundance of CYP2R1 compared

to the normal adjacent tissue. Immunostaining of OSCC tumor specimen with a nonspecific IgG served as negative control (Fig. 1).

We next examined CYP2R1 expression in OSCC-derived cell lines (SCC1, SCC11B, and SCC14a). Real-time RT-PCR analysis of total RNA isolated from these cells showed that $1,25(\text{OH})_2\text{D}_3$ (10^{-8} M) significantly increased CYP2R1 mRNA expression in these cells. SCC14a cells showed a high level of CYP2R1 mRNA expression compared to other cell lines SCC1 and SCC11B (Fig. 2a). Western blot analysis of total cell lysates further confirmed that $1,25(\text{OH})_2\text{D}_3$ stimulates CYP2R1 abundance (4.8-fold) in a time-dependent (0–72 h) manner in SCC14a cells (Fig. 2b). We next examined the vitamin D receptor (VDR) mRNA expression in OSCC cells. SCC14a cells were stimulated with $1,25(\text{OH})_2\text{D}_3$ (10^{-8} M) for 0–48 h, and total RNA isolated was subjected to real-time RT-PCR analysis for VDR mRNA expression. As shown in Fig. 2c, $1,25(\text{OH})_2\text{D}_3$ significantly increased (4.6-fold) VDR mRNA expression in a time-dependent manner. These results suggest that $1,25(\text{OH})_2\text{D}_3$ modulates VDR and CYP2R1 expression in OSCC tumor cells. We then tested the effect of $1,25(\text{OH})_2\text{D}_3$ on OSCC tumor cell growth. OSCC cells (SCC1, SCC11B, and SCC14a) were stimulated with $1,25(\text{OH})_2\text{D}_3$ (10^{-8} M) for 24 h and assayed for proliferation. As shown in Fig. 2d, $1,25(\text{OH})_2\text{D}_3$ significantly inhibit OSCC tumor cells proliferation.

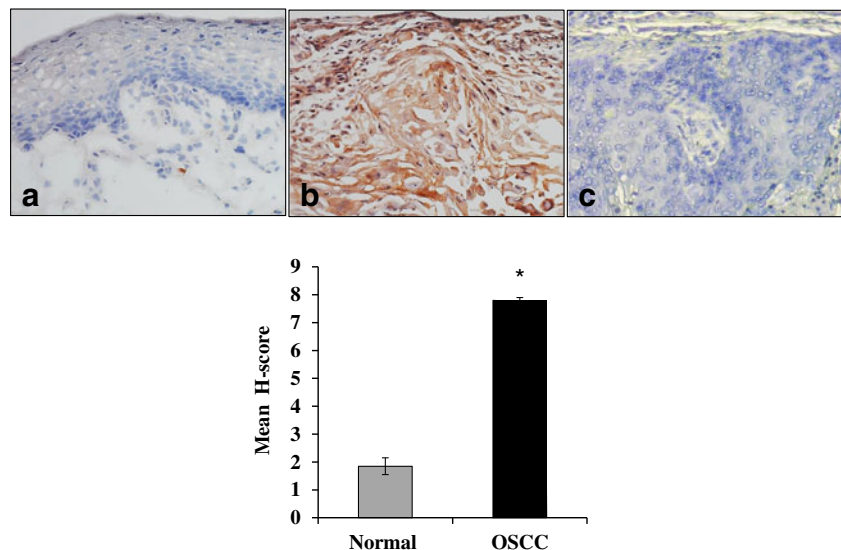
$1,25(\text{OH})_2\text{D}_3$ Transcriptional Control of CYP2R1 Gene Expression

To characterize the transcriptional control of human CYP2R1 gene expression in OSCC cells, we analyzed the CYP2R1 promoter region for potential transcription factor binding motifs by web-based TF search. We thus identified several AP-1 binding sites (–118, –245, and –1,318 bp) in the hCYP2R1

gene promoter (–2 kb relative to start codon) region. It has been shown that $1,25(\text{OH})_2\text{D}_3$ upregulates c-Jun/c-Fos (AP-1) expression in human osteosarcoma [41]. Therefore, we examined the $1,25(\text{OH})_2\text{D}_3$ modulation of c-Fos and c-Jun expression. SCC14a cells were stimulated with $1,25(\text{OH})_2\text{D}_3$ (10^{-8} M) for 0–6 h. Total cell lysates were subjected to western blot analysis for c-Fos and p-c-Jun expression. As shown in Fig. 3a, $1,25(\text{OH})_2\text{D}_3$ treatment increased the levels of c-Fos (5-fold) and p-c-Jun (7-fold) protein in a time-dependent manner in OSCC cells. Also, $1,25(\text{OH})_2\text{D}_3$ stimulation elevated (4.5-fold) JNK activity in these cells (Fig. 3b). Furthermore, $1,25(\text{OH})_2\text{D}_3$ treatment to OSCC cells transiently transfected with AP-1-luciferase reporter plasmid significantly increased (3.2-fold) AP-1 activity in these cells (Fig. 3c). We next examined the potential of AP-1 modulation of CYP2R1 gene expression in SCC14a cells. Cells were treated with JNK inhibitor SP 600125 (2 μM) for 30 min, followed by $1,25(\text{OH})_2\text{D}_3$ (10^{-8} M) for 48 h. Total RNA isolated from these cells was subjected to real-time RT-PCR analysis for CYP2R1 mRNA expression. As shown in Fig. 4a, JNK inhibitor significantly decreased $1,25(\text{OH})_2\text{D}_3$, inducing CYP2R1 mRNA expression in these cells.

We further examined the participation of JNK in $1,25(\text{OH})_2\text{D}_3$ transcriptional regulation of CYP2R1 gene promoter activity in SCC14a cells. PGL2 Basic-hCYP2R1 promoter-luciferase reporter plasmid was transiently transfected into SCC14a cells using the lipofectamine reagent. Cells were cultured with $1,25(\text{OH})_2\text{D}_3$ (10^{-8} M) in the presence or absence of JNK inhibitor for 48 h. Total cell lysates obtained from these cells were analyzed for luciferase activity as described. As shown in Fig. 4b, JNK inhibitor suppressed $1,25(\text{OH})_2\text{D}_3$ stimulation of hCYP2R1 gene promoter activity compared to unstimulated cells. Thus, our results suggest that AP-1 is a downstream regulator of vitamin D signaling to modulate CYP2R1 expression in OSCC tumor cells. We next,

Fig. 1 CYP2R1 abundance in human OSCC tumor specimens. Immunohistochemical staining of CYP2R1 expression in a representative **a** normal adjacent tissue, **b** OSCC tumor specimen, and **c** control IgG as analyzed by tissue microarray. The mean *H* score of OSCC and adjacent normal tissue from 60 to 14 specimens respectively is illustrated as a graph. The data are shown as mean \pm SD (* p < 0.05)



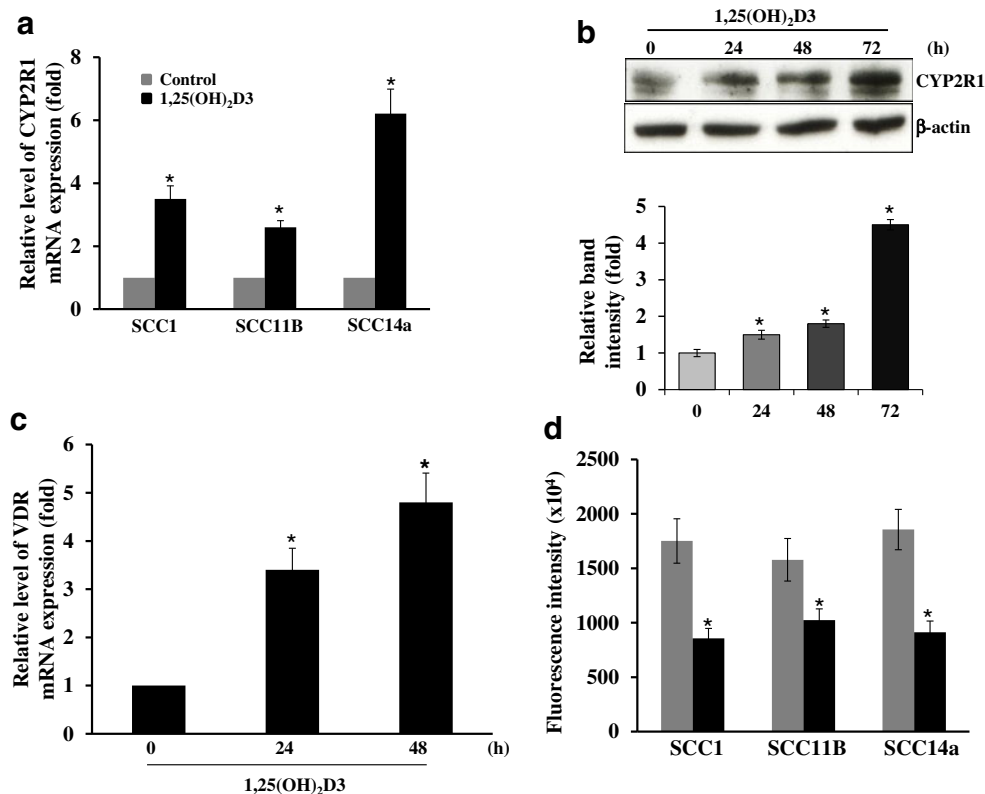


Fig. 2 1,25(OH)₂D₃ enhances CYP2R1 mRNA expression in OSCC cell lines. **a** OSCC tumor cell lines SCC1, SCC11B, and SCC14a cells were stimulated with 1,25(OH)₂D₃ (10⁻⁸ M) for 48 h. Total RNA isolated was subjected to real-time RT-PCR analysis for CYP2R1 mRNA expression. The relative levels of CYP2R1 mRNA expression were normalized with respect to the levels of GAPDH amplification. **b** SCC14a cells were stimulated with 1,25(OH)₂D₃ (10⁻⁸ M) for 0–72 h. Total cell lysates obtained were subjected to western blot analysis for CYP2R1 levels. β-actin levels served as loading control. The band intensity was quantified

by densitometric analysis using the NIH ImageJ Program. **c** SCC14a cells were stimulated with 1,25(OH)₂D₃ (10⁻⁸ M) for 0–48 h. Total RNA isolated was subjected to real-time RT-PCR analysis for VDR mRNA expression. The relative levels of VDR mRNA expression were normalized with respect to the levels of GAPDH amplification. **d** OSCC tumor cells were seeded (1×10⁴ cells/well) in a 96-well plate. Cells were stimulated with 1,25(OH)₂D₃ (10⁻⁸ M) for 24 h and incubated with alamarBlue reagent for 4 h at 37 °C and assayed for cell proliferation. Data represent triplicate studies and are shown as mean±SD (**p*<0.05)

delineate the link between JNK activation and vitamin D inhibition of OSCC tumor cell proliferation. SCC14a cells were treated with JNK inhibitor (2 μM) for 30 min, followed by 1,25(OH)₂D₃ (10⁻⁸ M) for 24 h. As shown in the Fig. 4c, JNK inhibitor significantly decreased vitamin D inhibition of OSCC cell proliferation. These data suggest the participation of JNK in anticancer activity of vitamin D.

Discussion

CYP2R1 is a microsomal vitamin D 25-hydroxylase. Although at least six CYP enzymes have been reported with 25-hydroxylase activity, CYP2R1 is the predominant type expressed at high levels in prostate and ovarian cancer cells [3, 8]. In this study, we demonstrated that human OSCC tumor cells express CYP2R1 at high levels and that physiologic concentrations of 1,25(OH)₂D₃ modulate CYP2R1 levels in these cells. OSCC have been shown to produce elevated levels

of several cytokines/growth factors such as PTH, TNF-α, IL-1, and TGF-β [31]. Therefore, it is possible that besides 1,25(OH)₂D₃, tumor-derived cytokines may regulate CYP2R1 levels in OSCC cells. Recent evidence indicates that dietary vitamin D and 1,25(OH)₂D₃ show equivalent anticancer activity in mouse xenograft models of breast and prostate cancer. 1,25(OH)₂D₃ deficiency increases the cancer risk and mortality [35]. Environmental factors such as sunlight exposure which promotes 1,25(OH)₂D₃ synthesis in skin lowers cancer risk [13, 37]. Furthermore, adequate levels of serum vitamin D are important to decrease the risk of prostate cancer [11]. Our findings that 1,25(OH)₂D₃ modulates CYP2R1 abundance in OSCC tumor cells suggest that vitamin D3 deficiency enhances the risk of oral cancer. Although an inverse association between dietary components such as folate and oral cancer prognosis is noted [30], the contribution of vitamin D metabolism in OSCC is yet to be established. Vitamin D has been implicated in cellular proliferation, differentiation, and apoptosis of normal and cancer cells [7, 12]. In addition, 1,25

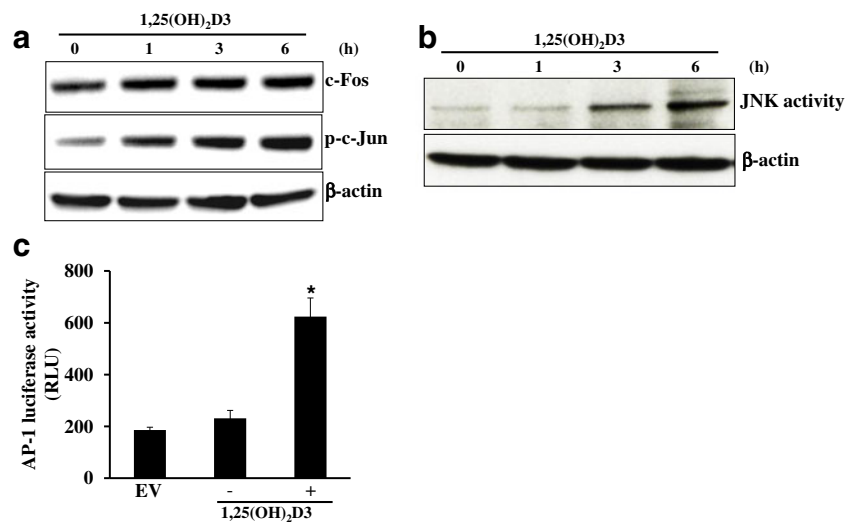


Fig. 3 1,25(OH)₂D₃ enhances c-Fos and p-c-Jun levels in SCC14a cells. **a** Cells were stimulated with 1,25(OH)₂D₃ (10⁻⁸ M) for indicated time point (0–6 h). Total cell lysates were subjected to western blot analysis for c-Fos and p-c-Jun levels. **b** SCC14a cells were stimulated with 1,25(OH)₂D₃ (10⁻⁸ M) for 0–6 h. Total cell lysates were assayed for JNK activity using a solid-phase GST-c-Jun (1–89 amino acids) fusion protein as described in “Materials and Methods.” **c** SCC14a cells were

transfected with empty vector (EV) and AP-1-luciferase reporter plasmids and stimulated with 1,25(OH)₂D₃ (10⁻⁸ M) for 48 h. Total cell lysates prepared were assayed for luciferase activity. The transfection efficiency was normalized by β-galactosidase activity co-expressed in these cells. Values are expressed as mean±SD for three independent experiments (**p*<0.05)

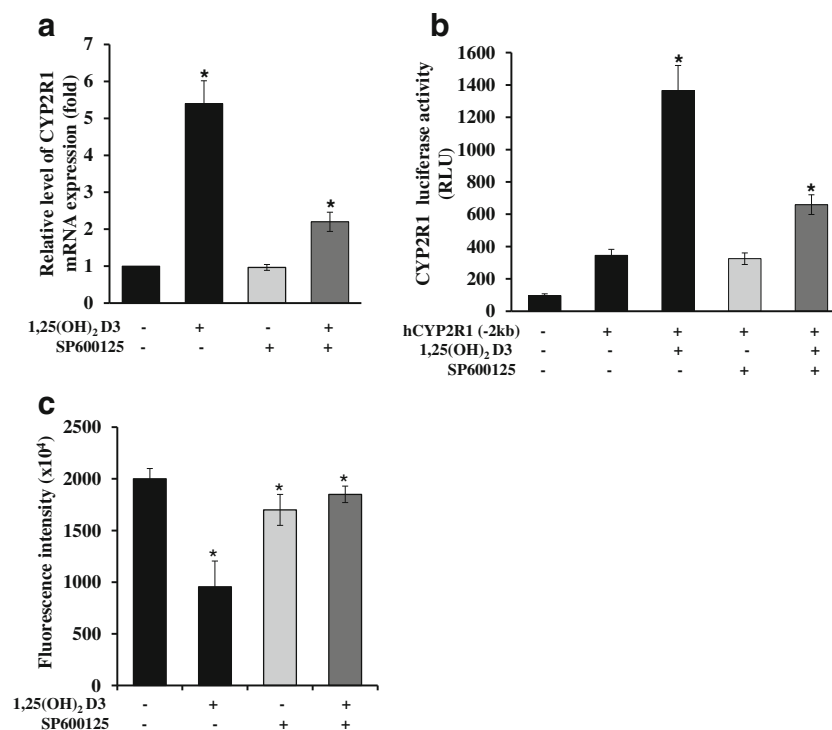


Fig. 4 Inhibition of JNK suppresses 1,25(OH)₂D₃-stimulated CYP2R1 expression in SCC14a cells. **a** Cells were treated with a 2-μM concentration of JNK inhibitor (SP600125) for 30 min, followed by stimulation with 1,25(OH)₂D₃ (10⁻⁸ M) for 48 h. Total RNA isolated was subjected to real-time RT-PCR analysis for CYP2R1 mRNA expression. The relative levels of CYP2R1 mRNA expression were normalized with respect to the levels of GAPDH amplification. **b** Cells were transfected with empty vector (EV) and pGL2 Basic-hCYP2R1 promoter-luciferase reporter plasmid and stimulated with 1,25(OH)₂D₃ (10⁻⁸ M) for 48 h in

the presence and absence of JNK inhibitor. Total cell lysates were assayed for luciferase activity. The transfection efficiency was normalized by β-galactosidase activity co-expressed in these cells. **c** JNK inhibitor suppresses vitamin D inhibition of OSCC cell proliferation. SCC14a cells were stimulated with 1,25(OH)₂D₃ (10⁻⁸ M) for 24 h in the presence and absence of JNK inhibitor (2 μM) and incubated with alamarBlue reagent for 4 h at 37 °C and assayed for cell proliferation. Data represent triplicate studies and are shown as mean±SD (**p*<0.05)

(OH)₂D₃ inhibits hepatocellular carcinoma through reducing inflammatory cytokines [16]. Recently, vitamin D status, intake, and metabolism are implicated in oral cancer risk [45]. Vitamin D activation and VDR binding has been shown to modulate TGF- β which exerts antiproliferative activity of cancer cells [21]. 1,25(OH)₂D₃ showed antiproliferative effect on thyroid cancer cell lines that demonstrated high levels of CYP2R1 expression [1]. CYP2R1 has been shown to be predominantly expressed in prostate cancer cells, suggesting that vitamin D metabolites play an important role in regulating prostate cancer growth [3]. Conversely, renal clear cell cancer cells showed suppression of VDR and CYP2R1 expression during malignant transformation [2]. Recently, 1,25(OH)₂D₃ has been shown to modulate several cytokine levels in plasma from patients with HNSCC [38]. Therefore, it is possible that 1,25(OH)₂D₃ regulation of cytokine/growth factor concentration in OSCC cells may affect the CYP2R1 gene expression in tumor cells.

Previously, a potential role for c-Jun and c-Fos protein levels in malignant transformation of oral mucosa has been reported [36]. Also, OSCC have been shown to constitutively express low levels of JNK activity [42]. NF- κ B has been shown to be constitutively activated in squamous cell carcinoma [22]. It has been reported that antiproliferative actions of 1,25(OH)₂D₃ involve VDR-mediated activation of MAPK signaling molecules and AP-1/p21waf1 upregulation in human osteosarcoma [41]. Evidence also indicates that patients with oral and pharyngeal cancers harbor polymorphisms and mutations in VDR [17]. Gene polymorphisms associated with VDR and other cytochrome P450 family members CYP27B1 and CYP24A1 may affect susceptibility to OSCC [43]. Although CYP2R1 gene promoter contains a putative vitamin D response element (−1,969 to −1,953 bp relative to start codon), our findings using JNK inhibitor confer the specificity for AP-1 transcription factor to enhance CYP2R1 abundance in OSCC cells. Previously, it has been reported that vitamin D₃ and 13-*cis* retinoic acid have equipotent antiproliferative effects on tongue squamous cell carcinoma (SCC-25) cells [9]. Also, 1,25(OH)₂D₃ has been shown to inhibit the growth of HNSCC cells through upregulation of cell cycle inhibitor p18 expression [14]. Consistently, we demonstrated that 1,25(OH)₂D₃ inhibits OSCC tumor cell proliferation. Furthermore, our results that JNK inhibitor blocks vitamin D inhibition of OSCC tumor cell proliferation suggest that c-Jun activation plays an important role in anticancer activity. Therefore, the vitamin D analogs may have an adjunctive role to play in the management of certain cancers [20, 40]. It has been shown that 5-FU and 13-*cis* retinoic acid combination potently inhibits OSCCs than 5-FU and vitamin D alone [6]. Recently, MART-10, a vitamin D analog has been shown to inhibit HNSCC cells growth [5]. Vitamin D effects may be cell line-specific, and lung adenocarcinoma cancer cells with distinct EGFR mutations have been shown to be more

responsive to vitamin D [44]. However, in this study, we demonstrated that vitamin D inhibits the growth of different OSCC tumor-derived cell lines. Thus, our results suggest that AP-1 is a downstream effector of 1,25(OH)₂D₃ signaling to modulate CYP2R1 expression and inhibits OSCC tumor cell proliferation. Therefore, the vitamin D analogs could be potential therapeutic agents to control OSCC tumor progression.

Acknowledgments We thank Dr. Alfredo A. Molinolo M.D., Ph.D, NIDCR, NIH, for providing the OSCC tumor tissue microarray slides.

Conflict of Interests The authors declare no conflict of interest.

References

- Bennett RG, Wakeley SE, Hamel FG, High RR, Korch C, Goldner WS (2012) Gene expression of vitamin D metabolic enzymes at baseline and in response to vitamin D treatment in thyroid cancer cell lines. *Oncology* 83(5):264–272
- Blomberg Jensen M, Andersen CB, Nielsen JE, Bagi P, Jorgensen A, Juul A, Leffers H (2010) Expression of the vitamin D receptor, 25-hydroxylases, 1 α -hydroxylase and 24-hydroxylase in the human kidney and renal clear cell cancer. *J Steroid Biochem Mol Biol* 121(1–2):376–382
- Chen TC, Sakaki T, Yamamoto K, Kittaka A (2012) The roles of cytochrome P450 enzymes in prostate cancer development and treatment. *Anticancer Res* 32(1):291–298
- Cheng JB, Levine MA, Bell NH, Mangelsdorf DJ, Russell DW (2004) Genetic evidence that the human CYP2R1 enzyme is a key vitamin D 25-hydroxylase. *Proc Natl Acad Sci U S A* 101(20):7711–7715
- Chiang KC, Yeh CN, Hsu JT, Chen LW, Kuo SF, Sun CC, Huang CC et al (2013) MART-10, a novel vitamin D analog, inhibits head and neck squamous carcinoma cells growth through cell cycle arrest at G0/G1 with upregulation of p21 and p27 and downregulation of telomerase. *J Steroid Biochem Mol Biol* 138:427–434
- Dalirsani Z, Farajnia S, Javadzadeh Y, Mehdipour M, Koozegari S (2012) The effects of 5-fluorouracil alone and in combination with 13-*cis* retinoic acid and vitamin D₃ on human oral squamous cell carcinoma lines. *J Contemp Dent Pract* 13(3):345–350
- Deeb KK, Trump DL, Johnson CS (2007) Vitamin D signalling pathways in cancer: potential for anticancer therapeutics. *Nat Rev Cancer* 7(9):684–700
- Downie D, McFadyen MC, Rooney PH, Cruickshank ME, Parkin DE, Miller ID, Telfer C, Melvin WT, Murray GI (2005) Profiling cytochrome P450 expression in ovarian cancer: identification of prognostic markers. *Clin Cancer Res* 11(20):7369–7375
- Enepekides DJ, Black MJ, White JH (1999) The independent and combined effects of RAR-, RXR-, and VDR-selective ligands on the growth of squamous cell carcinoma in vitro. *J Otolaryngol* 28(2):83–89
- Erdem NF, Carlson ER, Gerard DA, Ichiki AT (2007) Characterization of 3 oral squamous cell carcinoma cell lines with different invasion and/or metastatic potentials. *J Oral Maxillofac Surg* 65(9):1725–1733
- Flanagan JN, Young MV, Persons KS, Wang L, Mathieu JS, Whitlatch LW, Holick MF, Chen TC (2006) Vitamin D metabolism in human prostate cells: implications for prostate cancer chemoprevention by vitamin D. *Anticancer Res* 26(4A):2567–2572
- Flynn G, Chung I, Yu WD, Romano M, Modzelewski RA, Johnson CS, Trump DL (2006) Calcitriol (1,25-dihydroxycholecalciferol)

- selectively inhibits proliferation of freshly isolated tumor-derived endothelial cells and induces apoptosis. *Oncology* 70(6):447–457
13. Freedman DM, Dosemeci M, McGlynn K (2002) Sunlight and mortality from breast, ovarian, colon, prostate, and non-melanoma skin cancer: a composite death certificate based case-control study. *Occup Environ Med* 59(4):257–262
 14. Gedlicka C, Hager G, Weissenböck M, Gedlicka W, Knerer B, Kornfehl J, Formanek M (2006) 1,25(OH)₂Vitamin D₃ induces elevated expression of the cell cycle inhibitor p18 in a squamous cell carcinoma cell line of the head and neck. *J Oral Pathol Med* 35(8):472–478
 15. Goda T, Shimo T, Yoshihama Y, Hassan NM, Ibaragi S, Kurio N, Okui T, Honami T, Kishimoto K, Sasaki A (2010) Bone destruction by invading oral squamous carcinoma cells mediated by the transforming growth factor-beta signalling pathway. *Anticancer Res* 30(7):2615–2623
 16. Guo J, Ma Z, Ma Q, Wu Z, Fan P, Zhou X, Chen L et al (2013) 1, 25 (OH)₂D₃ inhibits hepatocellular carcinoma development through reducing secretion of inflammatory cytokines from immunocytes. *Curr Med Chem* 20(33):4131–4141
 17. Hama T, Norizoe C, Suga H, Mimura T, Kato T, Moriyama H, Urashima M (2011) Prognostic significance of vitamin D receptor polymorphisms in head and neck squamous cell carcinoma. *PLoS One* 6(12):e29634
 18. Johnson NW, Jayasekara P, Amarasinghe AA (2011) Squamous cell carcinoma and precursor lesions of the oral cavity: epidemiology and aetiology. *Periodontol* 2000 57(1):19–37
 19. Kraus JA, Dabbs DJ, Beriwal S, Bhargava R (2012) Semi-quantitative immunohistochemical assay versus oncotype DX(R) qRT-PCR assay for estrogen and progesterone receptors: an independent quality assurance study. *Mod Pathol* 25(6):869–876
 20. Krishnan AV, Trump DL, Johnson CS, Feldman D (2012) The role of vitamin D in cancer prevention and treatment. *Rheum Dis Clin North Am* 38(1):161–178
 21. Krueger C, Hoffmann FM (2010) Identification of retinoic acid in a high content screen for agents that overcome the anti-myogenic effect of TGF-beta-1. *PLoS One* 5(11):e15511
 22. Loercher A, Lee TL, Ricker JL, Howard A, Geoghegan J, Chen Z, Suwoo JB et al (2004) Nuclear factor-kappaB is an important modulator of the altered gene expression profile and malignant phenotype in squamous cell carcinoma. *Cancer Res* 64(18):6511–6523
 23. Ma Y, Yu WD, Hidalgo AA, Luo W, Delansorne R, Johnson CS, Trump DL (2013) Inecalcitol, an analog of 1,25D₃, displays enhanced antitumor activity through the induction of apoptosis in a squamous cell carcinoma model system. *Cell Cycle* 12(5):743–752
 24. Malodobra-Mazur M, Paduch A, Lebiada A, Konopacka M, Rogolinski J, Szymczyk C, Wierzgon J et al (2012) VDR gene single nucleotide polymorphisms and their association with risk of oral cavity carcinoma. *Acta Biochim Pol* 59(4):627–630
 25. Mao L, Hong WK, Papadimitrakopoulou VA (2004) Focus on head and neck cancer. *Cancer Cell* 5(4):311–316
 26. Mishra A, Bharti AC, Varghese P, Saluja D, Das BC (2006) Differential expression and activation of NF-kappaB family proteins during oral carcinogenesis: role of high risk human papillomavirus infection. *Int J Cancer* 119(12):2840–2850
 27. Molinolo AA, Hewitt SM, Amornphimoltham P, Keelawat S, Rangaeng S, Meneses Garcia A, Raimondi AR et al (2007) Dissecting the Akt/mammalian target of rapamycin signaling network: emerging results from the head and neck cancer tissue array initiative. *Clin Cancer Res* 13(17):4964–4973
 28. Nomura T, Shibahara T, Katakura A, Matsubara S, Takano N (2007) Establishment of a murine model of bone invasion by oral squamous cell carcinoma. *Oral Oncol* 43(3):257–262
 29. Pandravadu SN, Yuvaraj S, Liu X, Sundaram K, Shanmugarajan S, Ries WL, Norris JS, London SD, Reddy SV (2010) Role of CXCL chemokine ligand 13 in oral squamous cell carcinoma associated osteolysis in athymic mice. *Int J Cancer* 126(10):2319–2329
 30. Pelucchi C, Talamini R, Negri E, Levi F, Conti E, Franceschi S, La Vecchia C (2003) Folate intake and risk of oral and pharyngeal cancer. *Ann Oncol* 14(11):1677–1681
 31. Piva MR, de Souza LB, Martins-Filho PRS, Nonaka CF, de Santana Santos T, Souza Andrade ES, Piva D (2013) Role of inflammation in oral carcinogenesis (part II): CD8, FOXP3, TNF-alpha, TGF-beta and NF-kappaB expression. *Oncol Lett* 5(6):1909–1914
 32. Quan J, Johnson NW, Zhou G, Parsons PG, Boyle GM, Gao J (2012) Potential molecular targets for inhibiting bone invasion by oral squamous cell carcinoma: a review of mechanisms. *Cancer Metastasis Rev* 31(1–2):209–219
 33. Schwartz GG, Whitlatch LW, Chen TC, Lokeshwar BL, Holick MF (1998) Human prostate cells synthesize 1,25-dihydroxyvitamin D₃ from 25-hydroxyvitamin D₃. *Cancer Epidemiol Biomarkers Prev* 7(5):391–395
 34. Sundaram K, Mani SK, Kitatani K, Wu K, Pestell RG, Reddy SV (2008) DACH1 negatively regulates the human RANK ligand gene expression in stromal/preosteoblast cells. *J Cell Biochem* 103(6):1747–1759
 35. Swami S, Krishnan AV, Wang JY, Jensen K, Horst R, Albertelli MA, Feldman D (2012) Dietary vitamin D(3) and 1,25-dihydroxyvitamin D(3) (calcitriol) exhibit equivalent anticancer activity in mouse xenograft models of breast and prostate cancer. *Endocrinology* 153(6):2576–2587
 36. Turatti E, da Costa Neves A, de Magalhães MH, de Sousa SO (2005) Assessment of c-Jun, c-Fos and cyclin D1 in premalignant and malignant oral lesions. *J Oral Sci* 47(2):71–76
 37. Wagner CL, Taylor SN, Dawodu A, Johnson DD, Hollis BW (2012) Vitamin D and its role during pregnancy in attaining optimal health of mother and fetus. *Nutrients* 4(3):208–230
 38. Walker DD, Reeves TD, de Costa AM, Schuyler C, Young MR (2012) Immunological modulation by 1alpha,25-dihydroxyvitamin D₃ in patients with squamous cell carcinoma of the head and neck. *Cytokine* 58(3):448–454
 39. Williams HK (2000) Molecular pathogenesis of oral squamous carcinoma. *Mol Pathol* 53(4):165–172
 40. Woloszyńska-Read A, Johnson CS, Trump DL (2011) Vitamin D and cancer: clinical aspects. *Best Pract Res Clin Endocrinol Metab* 25(4):605–615
 41. Wu W, Zhang X, Zanello LP (2007) 1alpha,25-Dihydroxyvitamin D₃ antiproliferative actions involve vitamin D receptor-mediated activation of MAPK pathways and AP-1/p21(waf1) upregulation in human osteosarcoma. *Cancer Lett* 254(1):75–86
 42. Yunoki T, Kariya A, Kondo T, Hayashi A, Tabuchi Y (2013) The combination of silencing BAG3 and inhibition of the JNK pathway enhances hyperthermia sensitivity in human oral squamous cell carcinoma cells. *Cancer Lett* 335(1):52–57
 43. Zeljic K, Supic G, Stamenkovic Radak M, Jovic N, Kozomara R, Magic Z (2012) Vitamin D receptor, CYP27B1 and CYP24A1 genes polymorphisms association with oral cancer risk and survival. *J Oral Pathol Med* 41(10):779–787
 44. Zhang Q, Kanterewicz B, Shoemaker S, Hu Q, Liu S, Atwood K, Hersherberger P (2013) Differential response to 1alpha,25-dihydroxyvitamin D₃ (1alpha,25(OH)₂D₃) in non-small cell lung cancer cells with distinct oncogene mutations. *J Steroid Biochem Mol Biol* 136:264–270
 45. Kingsley K, Bergman C, Keiserman M, Mobley C (2013) Oral cancer risk and vitamin D status, intake and supplementation. *OA Cancer* 1:6